Hydrometallurgy 181 (2018) 206–214

Contents lists available at ScienceDirect

Hydrometallurgy

journal homepage: www.elsevier.com/locate/hydromet

Recovery of Zr, Hf, Nb from eudialyte residue by sulfuric acid dry digestion and water leaching with H_2O_2 as a promoter

Yiqian Ma[a], Srecko Stopic[a,*], Lars Gronen[b], Bernd Friedrich[a]

[a] Institute of Process Metallurgy and Metal Recycling (IME), RWTH Aachen University, Intzestraße 3, Aachen 52056, Germany
[b] Institute of Applied Mineralogy and Economic Geology, RWTH Aachen University, Wüllnerstraße 2, Aachen 52062, Germany

ARTICLE INFO

Keywords:
Eudialyte
Residue
Acid digestion
Leaching
Phase changes

ABSTRACT

Following the initial hydrometallurgical extraction of rare earth elements from the eudialyte mineral, the residue is known to contain additional valuable metals. In this reported study, a two-stage acidic treatment was investigated to extract Zr, Hf, Nb from the eudialyte residue. The objective was to obtain high recovery yields with a low consumption of acid, so the proposed preprocessing step was sulfuric acid dry digestion, which was held above the boiling point of water. The treated residue was then leached with water and H_2O_2 was added to promote the leaching of Zr, Hf and Nb. It was found that the H_2O_2 increased the oxidation potential of the acidic system, which assisted the decomposition of the mineral phases that contained Zr, Hf and Nb. In addition, the H_2O_2 acted as a reaction promoter by providing O_2^{2-} ions that formed complexes with the cations, shifted the reaction equilibrium and inhibited hydrolysis of Nb(IV). The QEMSCAN, XPS and SEM analysis were used to reveal the mineralogical characteristics of the solid samples. These characteristics demonstrated the chemical changes that occurred during extraction and helped to explain the mechanisms at work during the processes. The SEM analysis results showed that metals sulfate salts and quartz were present after the digestion process. The treated eudialyte residue leached the soluble salts into solution, whereas the quartz remained in the residue. After optimizing the treatment parameters by varying the process conditions it was found that the eudialyte extract produced 89.1% Zr, 81.2% Hf and 71.2% Nb and the most suitable process parameters were: digestion conditions: H_2SO_4/eudialyte residue: 25 ml/100 g, water/eudialyte residue: 20 ml/100 g, 110 °C, 4 h; leaching conditions: L/S: 3:1, H_2O_2/eudialyte residue: 10 ml/100 g, room temperature, 1 h.

1. Introduction

Eudialyte is a complex Na-Ca-zirconosilicate mineral that is generally rich in Fe, Al, Mn, Ti, K, Nb and contains attractive quantities of rare earth elements (REE) (Giuseppetti et al., 1971; Borst et al., 2016; Anthony et al., 2010). The typical empirical chemical formula for Eudialyte is $Na_4(Ca, Ce, Fe)_2ZrSi_6O_{17}(OH, Cl)_2$, but it displays a wide range of chemical compositions (Johnsen et al., 2003; Zakharov et al., 2011). Eudialyte is a potential REE resource, because of its good solubility in acid, low radioactivity and relatively high content of REE (Goodenough et al., 2016; Sadeghi et al., 2013; Sjöqvist et al., 2013). It is expected that more eudialyte will be mined as an alternative REE resource due to the popular demand for REE as essential materials for modern technologies (Krishnamurthy and Gupta, 2015; Alonso et al., 2012; Golev et al., 2014; Morais and Ciminelli, 2004). For example, the current EURARE project is tasked with studying the exploitation of promising REE resources in Europe including eudialyte minerals in Norra Kärr (Sweden) and Kvanefjeld (Greenland) (Goodenough et al., 2016; Balomenos et al., 2017).

Eudialyte can be directly decomposed by acid (Zakharov et al., 2011). According to some previous research, H_2SO_4 may not be the best candidate for REE extraction due to the formation of rare earth double sulfates (Voßenkaul et al., 2016; Kul et al., 2008). Meanwhile, it has been found that concentrated HCl can be used to efficiently extract REE from eudialyte concentrate, which can preclude the formation of silica gel (Voßenkaul et al., 2016; Davris et al., 2017), but only small quantities of Zr, Hf, Nb were leached from the mineral by this REE extraction. The HCl technology was used to extract REE from eudialyte concentrate in the EURARE project. The elements Zr, Hf, Nb either remained in the leach residue or were transferred back into the residue by precipitation. The resulting residue contained high quantities of Zr with trace amounts of Hf and Nb. The recovery of these metals from the eudialyte residue would undoubtedly increase the economic efficiency of the processing of this mineral.

* Corresponding author.
E-mail address: sstopic@ime-aachen.de (S. Stopic).

https://doi.org/10.1016/j.hydromet.2018.10.002
Received 28 March 2018; Received in revised form 17 August 2018; Accepted 2 October 2018
Available online 04 October 2018
0304-386X/

The best performance for extraction of Zr from eudialyte concentrate is ensured by the use of H_2SO_4. However, a sufficiently high extraction efficiency of Zr can be only be achieved when a large excess of acid is used (Zakharov et al., 2011) or by the introduction of potentially toxic fluoride ions (Dibrov et al., 2002; Litvinova and Chirkist, 2013). For example, Lebedev reported on a technology that was based on the two-stage decomposition of eudialyte concentrate using 50% H_2SO_4, but it was found that the recovery of Zr was less than 82% (Lebedev, 2003). Although the eudialyte residue in this study was initially treated with HCl, its Zr extraction performance was similar to the extraction from the eudialyte concentrate. In addition, extraction of Hf, Nb from the eudialyte has not been previously reported.

This study, proposes a novel flowchart for the extraction of Zr, Hf, Nb from the eudialyte residue with the goal of maximizing recovery yields with a minimum consumption of acid. Highly concentrated acid digestion represented the first step, which was followed by water leaching employing H_2O_2 as a promoter. The effects of the various parameters on the Zr, Hf, Nb recovery and the behavior of iron, aluminum and silica were studied. Moreover, the law of phase changes was illustrated.

2. Experimental

2.1. Materials and analysis

As a resource for REE, Eudialyte ore has been mined in South Greenland and the concentrated eudialyte used in this study was obtained from the Geological Survey of Finland (GTK) after beneficiation. Hydrochloric acid (HCl) was then used to leach REE from the eudilayte concentrate. It was found that about 30% Zr and Hf were leached from the mineral using the HCl. The remnant Zr and Hf were then treated like impurities similar to Fe and Al by treating the leach residue through neutralization using $CaCO_3$. The mixture of the eudialyte leach residue together with the impurity precipitation from the pilot-scale test was the initial material used in this study.

Analytical H_2SO_4 (96 wt%), H_2O_2 (30 wt%) and distilled water were used in the experiments. The composition of the solid samples was determined by XRF analysis (X-ray fluorescence), the key elements in the solid sample were analyzed after dissolving, and the elements present in the test solutions were identified using ICP-OES analysis (Peculiarity Optima 5300DV, Perkin Elmer). The mineral composition was determined by QEMSCAN analysis (Quantitative Evaluation of Materials by scanning electron microscopy). This analytical method enables an X-ray-based quantitative chemical mapping of the sample material and consists of a scanning electron microscope in combination with two energy-dispersive X-ray spectrometers. More than 40 elements were chosen for measurement base on prior conducted chemical analysis. The X-ray data were acquired and were assigned into suitable phases with a specific concentration range for each phase using idiscover© software. The accuracy of phase boundaries was verified by overlapping BSE images. For a better overview, phases with an amount less than 1 wt% and of minor interest were subsumed to other phases. X-ray photoelectron spectroscopy (XPS) measurements were performed on the samples using a monochromatic AlKα ($h\nu$ = 1486.6 eV) source with a Thermo Scientific ESCALAB 250 spectrometer. The C1s peak positioned at binding energy 285 eV was used to perform charge correction. High-resolution XPS scans were performed on the samples to identify the oxidation states of iron. Lorentzian-Gaussian curve fitting was employed to deconvolute the XPS spectra into separate peaks using XPSPEAK 4.1 software. The microstructure of the solid samples was examined using a Scanning Electron Microscope (SEM) – Jeo16380 LV. Energy dispersive X-Ray spectroscopy (EDS) was utilized to reveal elemental composition of the samples analyzed by SEM.

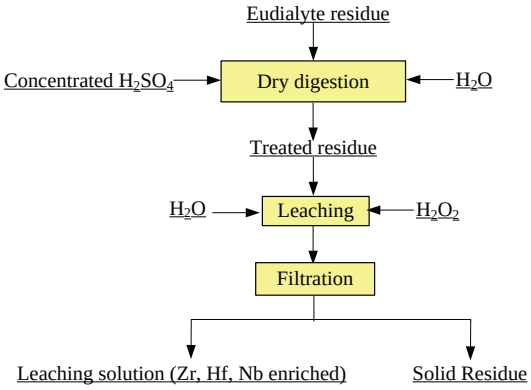

Fig. 1. Proposed flowchart for the acid recovery of Zr, Hf, Nb from eudialyte residue.

2.2. Extraction procedure

As shown in Fig. 1 the acid digestion process employing highly concentrated acid represented the first step. It is well known that digestion with concentrated acid at boiling temperatures always benefits the extraction of metals during a hydrometallurgical treatment (Vieceli et al., 2018; Davris et al., 2017). The mass of the eudialyte residue used in each experiment was 200 g. Some water was also added to the mixture to promote the ionization and diffusion of the sulfuric acid. The mixture was then held in a pre-heated oven at a temperature 110 °C for some time. Some of the reactions that occurred during the digestion can be expressed as follows (Davris et al., 2017; Terry, 1983; Zhang et al., 2016):

$$Na_{16}Ca_6Fe_2Zr_3Si_{26}O_{73}Cl_2 + 21H_2SO_4 + 33H_2O \rightarrow 7Na_2SO_4 + 6CaSO_4 + 2FeSO_4 + 3Zr(SO_4)_2 + 26Si(OH)_4 + 2NaCl \quad (1)$$

$$Zr(OH)_4 + 2H_2SO_4 \rightarrow Zr(SO_4)_2 + 4H_2O \quad (2)$$

$$2NaAlSi_3O_8 + 4H_2SO_4 + 16H_2O \rightarrow Na_2SO_4 + 6Si(OH)_4 + Al_2(SO_4)_3 \quad (3)$$

$$Si(OH)_{4(aq)} \rightarrow SiO_{2(s)} + 2H_2O_{(g)} \quad (4)$$

The relationship between $\Delta_rG_m^\theta$ and T of the reaction (4) is $\Delta_rG_m^\theta = -27.919\text{-}9.907E^{-4}T$, and the relationship between $lg(pH_2O/p^\theta)$ and 1/T is $lg(pH_2O/p^\theta) = -4109.65/T + 7.89$ ($\Delta_rG_m^\theta$: the standard reaction Gibbs energy, pH_2O: the partial pressure of H_2O (g), p^θ: the standard pressure) (Zhang et al., 2016; HSC chemistry 6.0). It is known that high temperature in a water-starved system promotes Reaction (4). Similarly, the compounds $Hf(SO_4)_2$ and $Nb_2O_3(SO_4)_2$ are expected to form after the acid digestion. Specified amount of water was subsequently added to the treated residue, which produced the leaching of Zr, Hf, Nb. During this leaching, some H_2O_2 was added to promote the process. It is well known that H_2O_2 is a strong oxidant. As a result, Fe^{2+} will be oxidized by the H_2O_2 to Fe^{3+} in solution. Iron is always present in the phases that contain Zr, Hf, Nb and Fe^{2+} is predominant species of iron in the eudialyte residue. Therefore, H_2O_2 could promote the dissolution of Fe from the residue, which will impact the extraction of Zr, Hf and Nb. Furthermore, O_2^{2-} can form complexes with Zr^{4+}, Hf^{4+} and Nb^{5+} in the solution (Bayot and Devillers, 2006; Gao et al., 2004;). Fig. 2 shows the *E*-pH diagrams of various systems. The related thermodynamics data were obtained from HSC chemistry 6.0 (HSC Chemistry 6.0, 2006) and metal compounds database (Smith and Martell, 1998). As can be seen, Nb^{5+} is easy to hydrolyze even under low pH, and the formation of the complexes can opportunely prevent its hydrolysis. In terms of the Zr and Hf, the formation of complexes of these metal ions can expand the stable region of dissolved Zr and Hf.

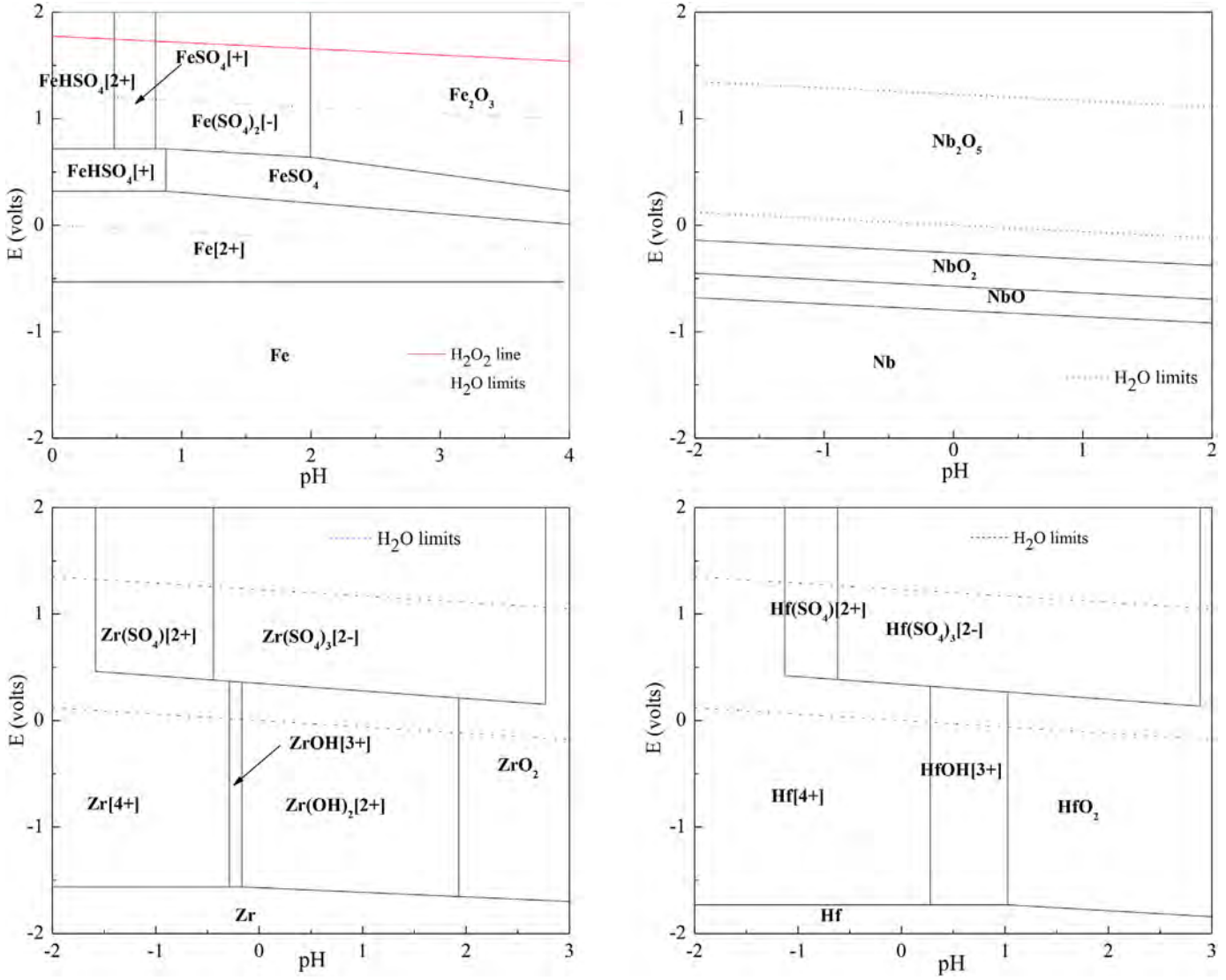

Fig. 2. *E*-pH diagram of the systems Fe-H_2O, Nb-H_2O, Zr-SO_4^{2-}–H_2O and Hf-SO_4^{2-}–H_2O at 298.15 K and low pH (Activities: Fe of 0.1, Nb of 0.01, Zr of 0.1, Hf of 0.01, SO_4^{2-} of 1.0 and H_2O_2 of 1.0). Note: sulfur compounds with low oxidation state are ignored.

The reactions described by (5)–(8) are some of the possible reactions that may occur in the oxidative leach stage (Bayot and Devillers, 2006; Gao et al., 2004; Yang et al., 2015):

$$4Zr(SO_4)_2 + 20H_2O + 2H_2O_2 \rightarrow [Zr_4(O_2)_2(OH)_4(H_2O)_{16}]^{8+} + 8HSO_4^- \quad (5)$$

$$4Hf(SO_4)_2 + 20H_2O + 2H_2O_2 \rightarrow [Hf_4(O_2)_2(OH)_4(H_2O)_{16}]^{8+} + 8HSO_4^- \quad (6)$$

$$Nb_2O_3(SO_4)_2 + 8H_2O_2 \rightarrow 2Nb(O_2)_4^{3-} + 8H^+ + 2HSO_4^- + 3H_2O \quad (7)$$

$$2FeSO_4 + 3H^+ + H_2O_2 \rightarrow 2Fe^{3+} + 2H_2O + HSO_4^- \quad (8)$$

After filtration and washing of the filter cake, a Zr, Hf, Nb enriched solution and solid residue were obtained. The composition of the leaching solution was analyzed to estimate the extraction efficiency.

3. Results and discussion

3.1. Characterization of eudialyte residue

The chemical composition of the eudialyte residue is given in Table 1 which shows Zr, Hf and Nb accounted for 6.26%, 0.22% and 0.53%, respectively. The phase composition of the eudialyte residue was complicated and some compounds were amorphous. The QEMSCAN analysis can help identify the phase associations and perform elemental mapping of the sample. Fig. 3 shows the phase distribution of the eudialyte residue by false color imaging and the right image is the BSE image. The results of the phase quantification are summarized in Fig. 4. Eudialyte phase described here represents Zr—Nb eudialyte group minerals as there is a group of minerals referred to as eudialyte for which the crystal chemistry has substantial variation. As can be seen from figures, 2.0% of the eudialyte phase was left in the residue after the REE extraction. The major phase in the material was partially leached eudialyte, which means that the eudialyte was not completely decomposed during the REE extraction. Eudialyte leach residue was the phase that remained after the decomposition of the eudialyte together with compounds formed during neutralization. These included siliceous secondary precipitation and hydrolysis

Table 1
Chemical composition of eudialyte residue.

Element	Zr	Hf	Nb	Al	Fe	Si	Ca	TREE
Content (% w/w)	6.26	0.22	0.53	4.98	3.21	25.52	2.19	0.2

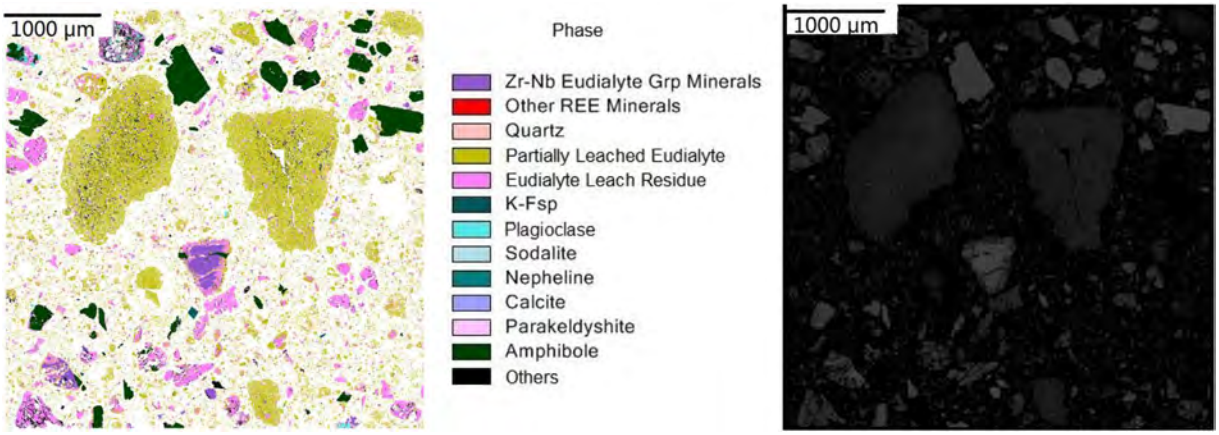

Fig. 3. QEMSCAN analysis of eudialyte residue before grinding (left: false color image, right: initial BSE-image) (K-Fsp: orthoclase and microcline).

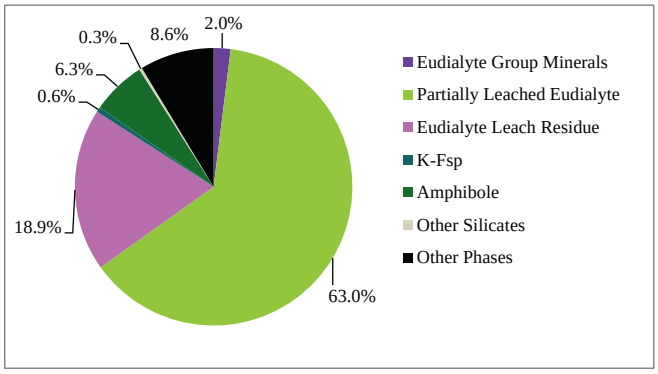

Fig. 4. Phase distribution of the eudialyte residue.

Table 2
Major identified phases and their elemental composition.

Phase	Major elements	Minor elements
Eudialyte group minerals	Si, O, Ca	Na, Fe, K, Zr, Hf, Mn, Nb, REE
Eudialyte leach residue	Si, O	Na, Al, Ca, Fe, K, Zr, Hf, Nb
Partially leached eudialyte	Si, O	Na, Ca, Fe, K, Zr, Hf, Nb,
K- Fsp	Al, O, Si, Na, K, Ca	Fe, K
Amphibole	Na, Si, Fe, O	K

products. The qualitative major elemental compositions of the identified phases are presented in Table 2. The target elements, Zr, Hf and Nb, were found primarily in eudialyte group minerals, partially leached eudialyte and eudialyte leach residue.

Due to the presence of trace amounts of Hf and Nb in the eudialyte residue, obtaining their elemental mappings is not informative for this material. The element Zr is the main target of the extraction due to its relatively high content and Zr elemental mapping of eudialyte residue is shown in Fig.5. The field scan image of eudialyte residue showed that Zr in the eudialyte residue was inhomogeneous and was present at a maximum content of around 15%.

Based on the study of the crystal chemistry of eudialyte group minerals, the Fe atoms present in the eudialyte phase are mostly in the +2 oxidation state. However, partially hydrated samples of the eudialyte phase appear to have a greater Fe^{3+}/Fe content (Khomyakov et al., 2010; Schilling et al., 2011). In Table 2, it can be seen that iron is always present with the target elements in the main identified phases in the eudialyte residue. Likewise, Nb appears in different valence states while Zr and Hf only exist in +4 state. X-ray photoelectron spectroscopy (XPS) was performed to investigate the overall oxidation states of Fe and Nb in the residue. As shown in Fig. 6 (a), the main and the

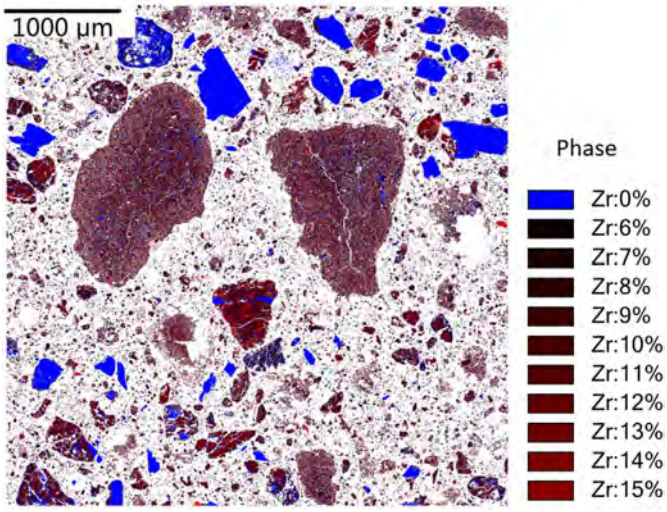

Fig. 5. Zr elemental mapping of the eudialyte residue by QEMSCAN analysis.

satellite binding energy positions of the Fe2p are closely related to those reported in literature (Aronniemi et al., 2005). The 2p3/2 and 2p1/2 emissions can be attributed to contributions of Fe^{2+} and Fe^{3+}. The XPS peaks of Fe2p3/2 and Fe2p1/2 are located at central positions ~710 eV and ~713 eV, respectively, and the green and blue lines show their satellite peaks. Furthermore, the area of the peak is positively correlated with the content of the different states, thus it was concluded that the Fe atoms were predominantly in +2 oxidation state in the eudialyte residue. In the Nb3d spectrum (Fig. 6(b)), two distinct peaks at binding energies of ~207 eV for Nb3d5/2 and ~210 eV for Nb3d3/2 are observed, which corresponds to the characteristic of Nb^{5+} ions in their oxide form (Dai et al., 2015). Therefore, the Nb atoms were in +5 oxidation state in the eudialyte residue.

3.2. Preliminary results

Some preliminary tests were performed to compare direct leaching, with water leaching after acid dry digestion. The parameters for these comparative experiments are shown in Table 3. As shown, no acid dry digestion was performed in experiments No. 1 and No. 2, but was performed in experiments No. 3 and No. 4 with the same amount of acid. In addition, the effect of H_2O_2 was also investigated preliminarily by performing experiments with and without addition of H_2O_2 during the leaching process. As seen from Fig. 7, experiments No. 3 and No. 4 exhibited a higher extraction efficiency for Zr than experiments No.1 and No. 2. These results mean that acid dry digestion at high

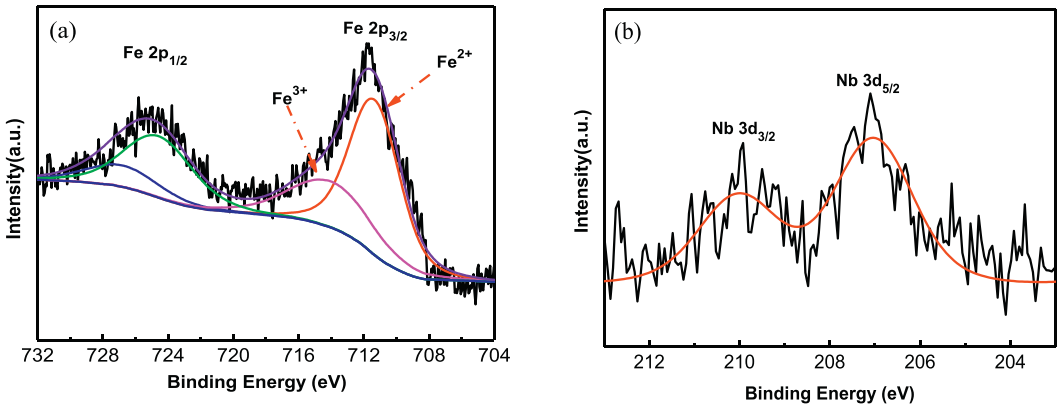

Fig. 6. XPS spectrum of the eudialyte residue. (a) Fe2p core peaks. (b) Nb3d core peaks.

Table 3
Preliminary experiment.

No.	Concentrated acid digestion (110 °C, 4 h)		Leaching (L/S = 2:1, 1 h)		
	H_2SO_4/ residue (mL/g)	H_2O/ residue (mL/g)	H_2SO_4/ residue (mL/g)	H_2O_2/ residue (mL/g)	Temperature (°C)
1	–	–	20/100	–	25
2	–	–	20/100	20/100	25
3	20/100	20/100	–	–	25
4	20/100	20/100		20/100	25

(H_2SO_4: 96 wt%, H_2O_2: 30 wt%)

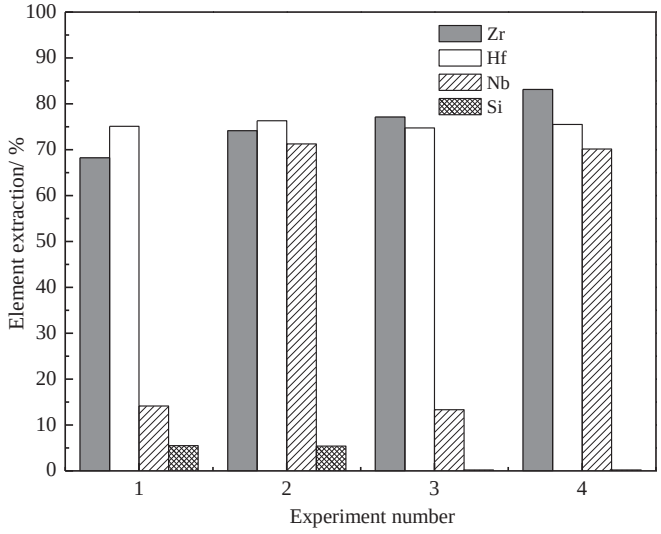

Fig. 7. Comparative results of preliminary extraction experiments.

temperature can enhance the extraction of Zr which represents the main valuable element in the residue. Thus, it is possible to reduce the consumption of acid with this pretreatment when compared to previous research (Lebedev, 2003). Furthermore, the acid digestion can reduce the dissolution of Si. The behavior of Si in these experiments agrees with the results reported elsewhere for the extraction of metals from materials with high silicon content (Kazadi et al., 2016; Zhang et al., 2016). Comparing test No. 1 with No. 2 or test No. 3 with No. 4, it can be seen that the addition of H_2O_2 produced positive results for the extraction of Zr and Nb, and particularly for the Nb to give a nearly fivefold increase in extraction efficiency. The effect of the main process parameters were studied further as a result of these initial comparative

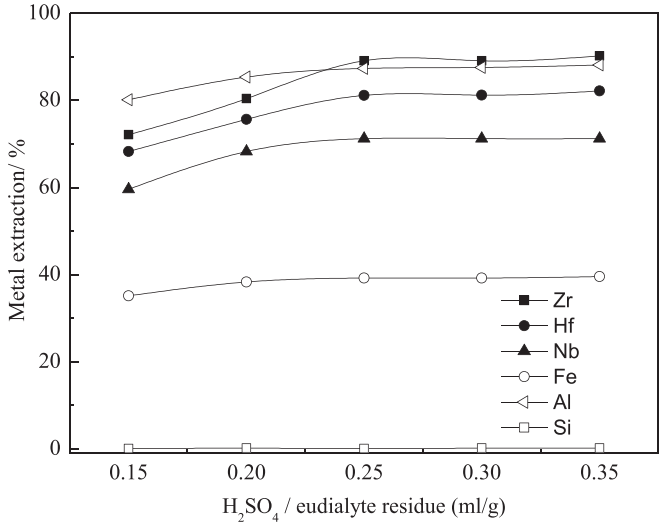

Fig. 8. Effect of H_2SO_4/eudialyte (ml/g) ratio on the extraction of elements from eudialyte, digestion conditions: 110 °C, 4 h, water/eudialyte residue: 20 ml/100 g, leaching conditions: L/S: 3:1, H_2O_2/eudialyte residue: 10 ml/100 g, room temperature, 1 h.

tests.

3.3. Acid digestion

3.3.1. Effect of acid quantity

As can been seen from Fig.8, extraction efficiency of the Zr, Hf, Nb, Fe and Al increased with the increase in acid/solid ratio. The dissolution of Si was very low in all cases. It should be noted that the quantity of sulfuric acid used represents one of the main process costs. Excessive quantities of acid requires large quantities of a basic agent to neutralize when recovering the metals from the leaching solution. Therefore, these data indicate that the most suitable ratio of acid to eudialyte residue should be 0.25 ml/g, since a ratio higher than this produced no appreciable increase in the extraction of Zr, Hf, Nb extraction.

3.3.2. Effect of water on digestion process

Some water is needed in the digestion process, because it can benefit uniform mixing and promote the ionization and diffusion of the sulfuric acid. Fig. 9 shows the experimental results for various H_2O/eudialyte (ml/g) ratios in the elemental extraction process. It was found that the addition of water had little effect on the dissolution of the Nb, Fe, Si. However, the efficiencies of the Zr, Hf and Al extractions increased with the addition of water from 0 to 0.2 ml per 1 g eudialyte residue. Further increases in the amount of water added did not increase the extraction

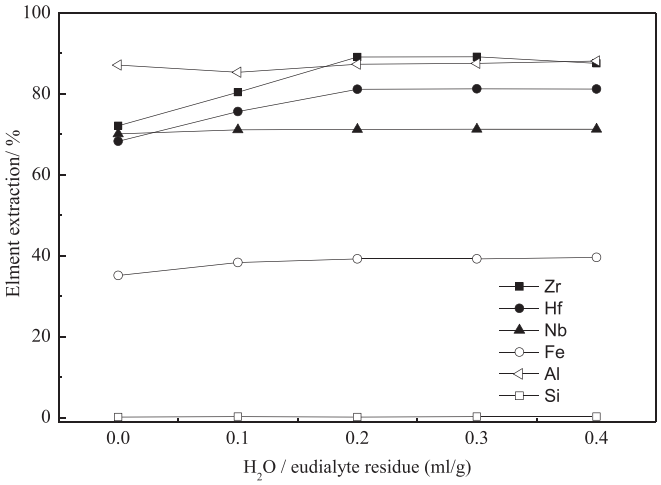

Fig. 9. Effect of H_2O/eudialyte residue (ml/g) ratio on extraction of elements from eudialyte, digestion conditions: 110 °C, 4 h, H_2SO_4/eudialyte residue: 25 ml/100 g, leaching conditions: L/S: 3:1, H_2O_2/eudialyte residue: 10 ml/100 g, room temperature, 1 h.

efficiency, but appeared to produce difficulty in mixing. Hence, a ratio of 0.2 ml of H_2O/ g eudialyte was chosen as the most suitable ratio for water addition to the process.

3.3.3. Effect of digestion time

The effect of digestion time on the extraction was also determined experimentally (Fig. 10). In these experiments the water/eudialyte residue ratio and H_2SO_4/eudialyte residue ratio were set at their optimum values, and it can be seen from the results in Fig. 10 that the extraction of all metals increased with prolonged reaction time. However, the extraction of Si exhibited an inverse relationship to reaction time. These results indicated that adequate dry digestion contributes to the chemical transformation of Si into the insoluble form, so a slow dissolution of Si occurs during leaching. The extraction performance of the system did not change with reaction times longer than 4 h, so the optimum digestion time was chosen to be 4 h.

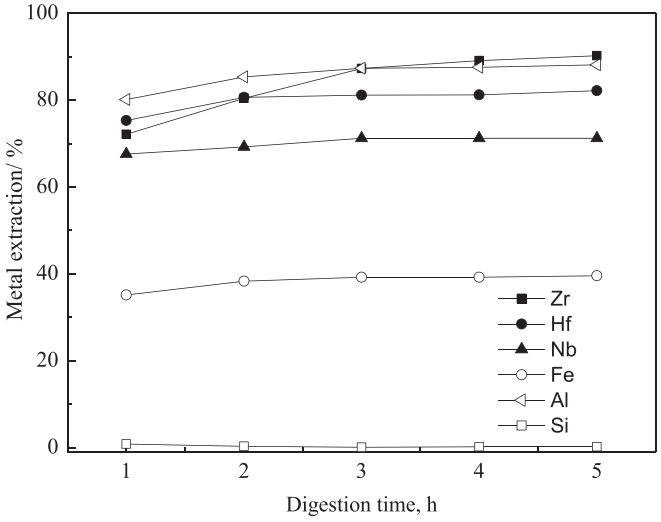

Fig. 10. Effect of digestion time on the extraction of elements from eudialyte, digestion conditions: 110 °C, water/eudialyte residue: 20 ml/100 g, H_2SO_4/eudialyte residue: 25 ml/100 g, leaching conditions: L/S: 3:1, H_2O_2/eudialyte residue: 10 ml/100 g, room temperature, 1 h.

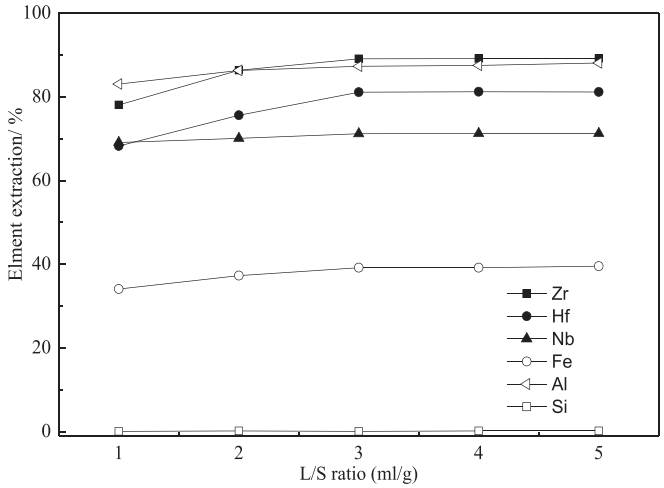

Fig. 11. Effect of L/S ratio on the extraction of elements from eudialyte, digestion conditions: 110 °C, 4 h, water/eudialyte residue: 20 ml/100 g, H_2SO_4/eudialyte residue: 25 ml/100 g, leaching conditions: H_2O_2/eudialyte residue: 10 ml/100 g, room temperature, 1 h.

3.4. Leaching procedure

3.4.1. Effect of liquid-solid ratio

After H_2SO_4 digestion under the most suitable conditions, the effect of varying the liquid/solid ratio during leaching was examined. As the data in Fig. 11 show, the extraction efficiency of the metals increased with the increase in the L/S ratio. The Zr extraction efficiency increased from 80% to 89% when the L/S ratio was increased from 1:1 ml/g to 3:1 ml/g, and above 3:1 ml/g, no further increase was noted. Considering that producing large quantities of leach solution would be detrimental to subsequent treatment, a L/S ratio of 3:1 ml/g was chosen as the suitable parameter for the process.

3.4.2. Effect of H_2O_2 quantity

The experimental results shown in Fig. 12 verify that H_2O_2 played the role of a promoter in the Zr, Hf, Nb extraction, and an increase in the extraction of Nb by the presence of H_2O_2 was particularly noteworthy. The dissolution of Fe was also increased by the H_2O_2. The results suggest that 0.1 ml H_2O_2 per gram eudialyte residue was sufficient

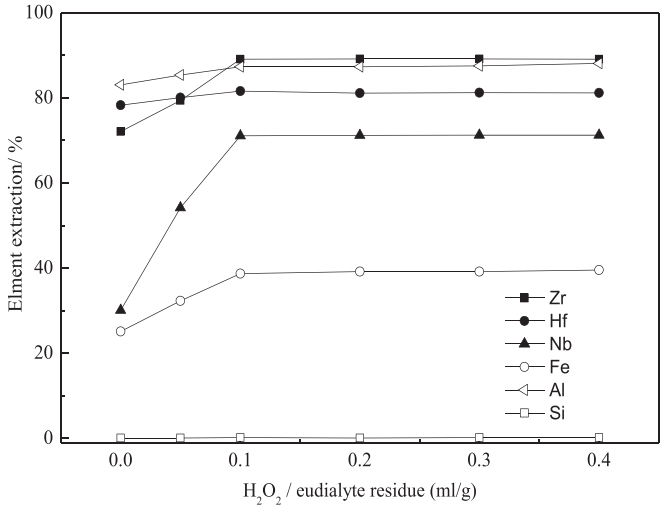

Fig. 12. Effect of H_2O_2 quantity on the extraction of elements from eudialyte, digestion conditions: 110 °C, 4 h, water/eudialyte residue: 20 ml/100 g, H_2SO_4/eudialyte residue: 25 ml/100 g, leaching conditions: L/S: 3:1, room temperature, 1 h.

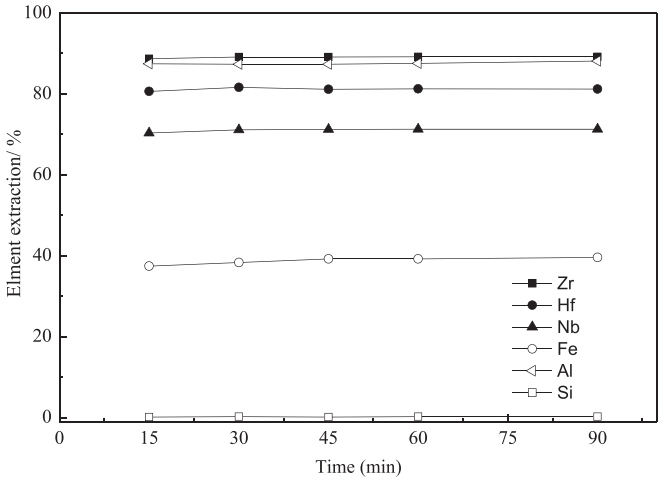

Fig. 13. Effect of leaching time on the extraction of elements from eudialyte, digestion conditions: 110 °C, 4 h, water/eudialyte residue: 20 ml/100 g, H_2SO_4/eudialyte residue: 25 ml/100 g, leaching conditions: H_2O_2/eudialyte residue: 10 ml/100 g, L/S: 3:1, room temperature.

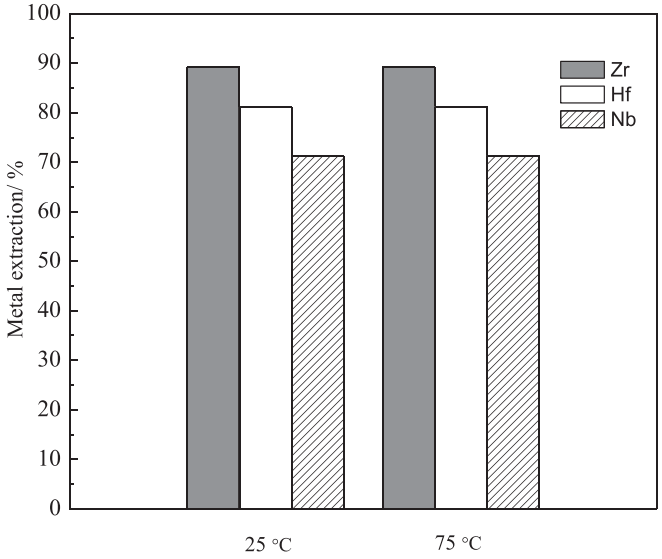

Fig. 14. Effect of leaching temperature on the extraction of elements from eudialyte, digestion conditions: 110 °C, 4 h, water/eudialyte residue: 20 ml/100 g, H_2SO_4/eudialyte residue: 25 ml/100 g, leaching conditions: H_2O_2/eudialyte residue: 10 ml/100 g, L/S: 3:1, 1 h.

Table 4
EDS analyses of the eudialyte residue.

Element (% w/w)	Na	Ca	Al	Fe	Zr	Hf	Nb	Si	K	Cl
Spot A	0.9	3.4	10.6	1.8	14.6	0.1	1.5	57.4		9.8
Spot B	14.7	0.4	1.6	26.2	–	–	–	52.7	3.2	–
Spot C	2.0	3.5	8.2	2.3	12.8	–	1.6	58.9	–	10.5

to produce a positive impact on the process, so that this amount was considered to be the most suitable.

3.4.3. Effect of leaching time and temperature

In previously reported research (Zhang et al., 2016; Kazadi et al., 2016) it was demonstrated that leaching time and temperature are not key variables in the behavior of the treated material after acid digestion, since this is mainly a process of salt dissolution. The experimental results of this study suggested that the same situation existed in our process. As shown in Fig. 13, the leaching efficiency of all the elements reached their maximum values in short time and longer reaction times did not increase the extraction efficiency. Thus 30 min was enough time for the water leaching process. Fig. 14 compares the results of leaching at 25 °C (room temperature) and 80 °C. The results show that it is not necessary to conduct the leaching at high temperature. Thus, room temperature water leaching was the reasonable choice.

Table 5
EDS analyses of the treated residue after H_2SO_4 digestion.

Element (% w/w)	Na	Ca	Al	Fe	Zr	Hf	Nb	Si	O	S
Spot A	–	–	0.9	0.6	0.8	–	–	32.6	53.6	2.7
Spot B	–	–	0.6	1.2	17.9	0.6	2.2	2.9	44 0.5	13.4
Spot C	–	–	10.1	0.5	2.0	–	–	2.9	54.0	28.4

Table 6
EDS analyses of the final residue after water leaching.

Element (% w/w)	Na	Ca	Al	Fe	Zr	Hf	Nb	Si	K	S
Spot A	0.6	0.4	1.8	0.5	3.8	–	0.7	86.9	–	5.5
Spot B	14.7	0.4	1.6	26.2	–	–	–	52.7	3.2	0.3

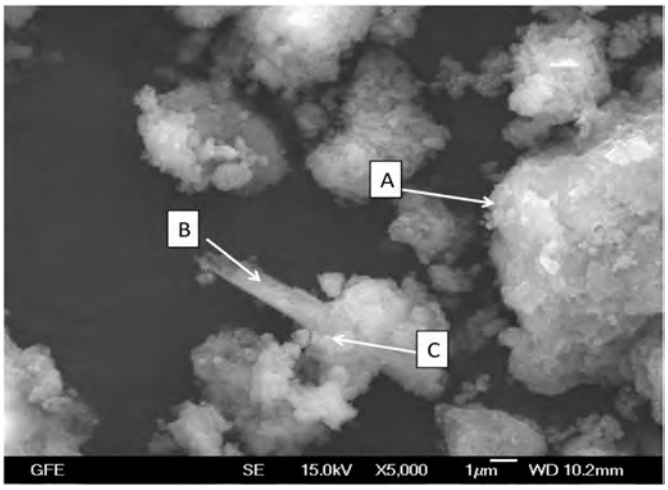

Fig. 15. SEM image of the eudialyte residue.

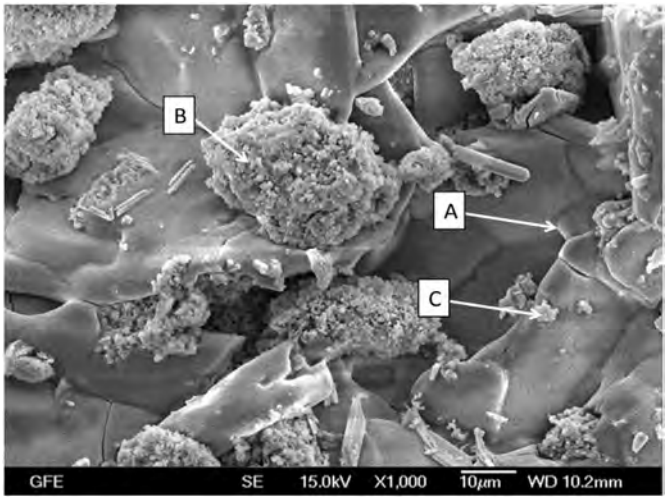

Fig. 16. SEM image of the treated residue after digestion with H_2SO_4.

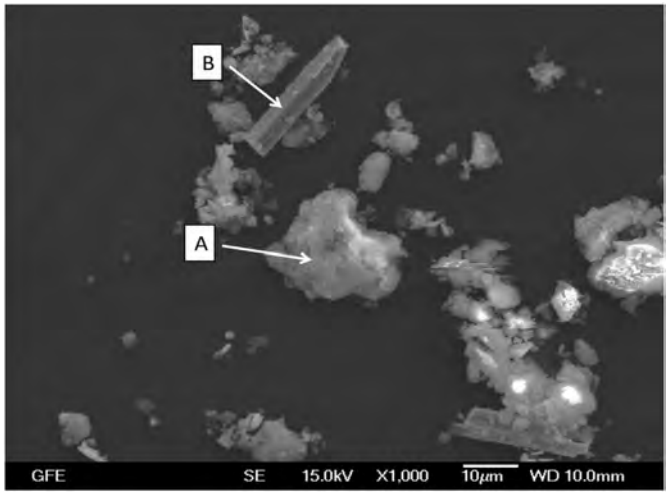

Fig. 17. SEM image of the final residue after water leaching.

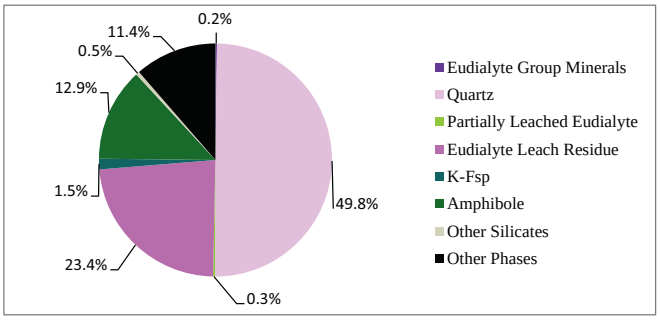

Fig. 19. Phase distribution in the final residue after extraction of Zr, Hf, Nb.

3.5. Morphology characterization and phase changes

Eudialyte residue, treated residue after H_2SO_4 digestion and final residue after water leaching were all characterized in a similar manner using SEM analysis. The changes in the morphology of the samples were observed by the SEM, and the compositions of select regions of the samples which revealed some changes in phase, were analyzed by EDS (Table 4–6).

In Fig. 15, it can be seen that the particles of eudialyte residue had irregular sizes and there was significant agglomeration of these particles This can be explained by the fact that silica precipitation occurred during the HCl treatment. According to Table 4, Fe, Al, Ca, Na, Si were found in all the particles, Spots A and C represent grains containing eudialyte phase or partially leached eudialyte with high content of Zr, Hf,Nb. In spot B. It can also be seen that there are some particles, which could an amphibole based on the results of QEMSCAN. These particles were wrapped by Fe/Al precipitate with some amorphous silica, and the Fe content was very high.

The SEM images of the treated residue after H_2SO_4 digestion indicated that distinct changes had occurred, as seen in Fig. 16. The treated residue tended to be chunky with some grains on the surface. Some crystals containing zirconium, hafnium, niobium sulfate salts

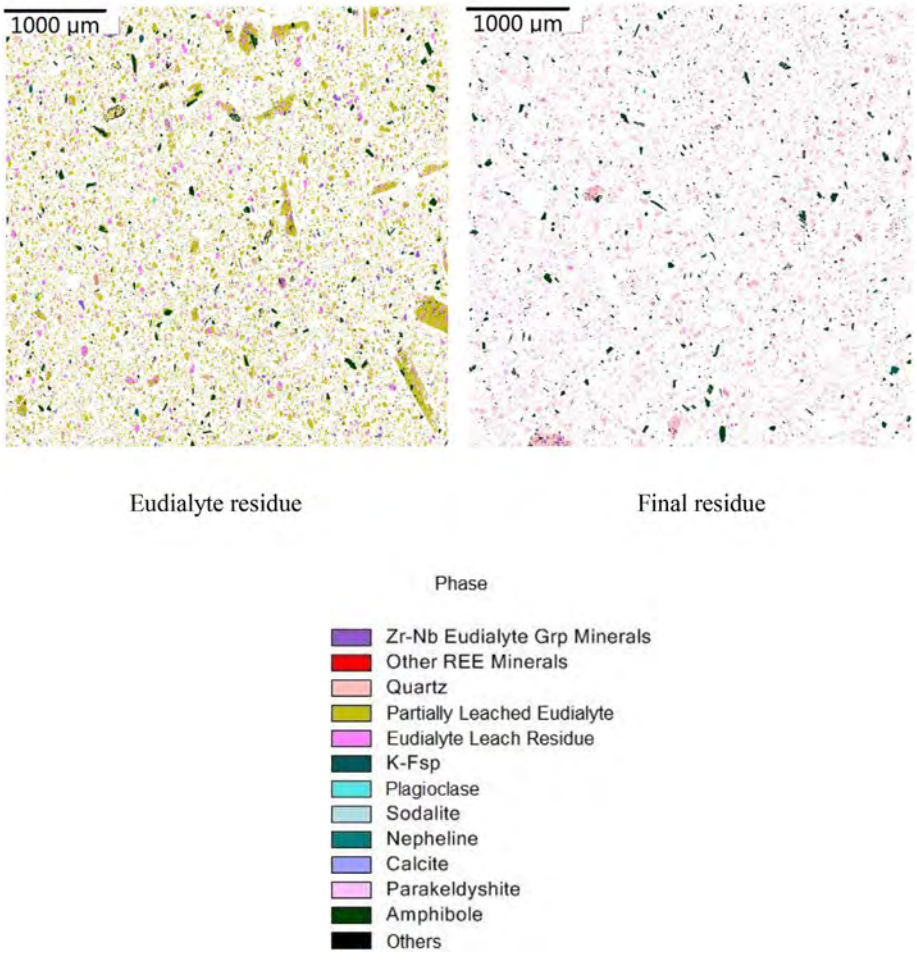

Fig. 18. QEMSCAN of the eudialyte residue and the final residue after extraction of Zr, Hf, Nb.

were found, and other sulfate salts containing iron and aluminum appeared to have formed as well (Table 5). The spot A consisted mainly of Si and O, which could well have been classified as quartz. The images also show that some grains were covered with a silica layer, which could potentially hamper acid diffusion. This may explain the poor and incomplete recovery of the Zr, Hf, Nb.

The SEM images and EDS analyses of the final residue after water leaching are shown in Fig. 17 and Table 6. The particles maintained their high content of Si. In the final residue the content of S was greatly decreased and very little Zr, Hf and Nb were detected It was found that needle grains (spot B) with high contents of Fe were present in the residue, indicating that some amphibole may not have decomposed.

The distribution of minerals in the eudialyte residue and in the final residue after water leaching were also compared (Fig. 18). As can be seen in Fig. 19, the results of the QEMSCAN analysis corresponded with the behavior of the Zr, Hf, Nb extraction. This indicated that a nearly total decomposition had occurred in the eudialyte phase, partially leached eudialyte phase, and the main phases in the final residue, were quartz, eudialyte leach residue, and amphibole.

4. Conclusions

A two-stage process was developed to recover Zr, Hf and Nb from an eudialyte residue after extracting the REE. The pretreatment, which was dry digestion with concentrated acid, was found to enhance the recovery process with a significant improvement to Zr extraction. The promotion of Hf and Nb extractions by the dry digestion is not significant while the dissolution of Si was significantly decreased. Based on the characterization of the eudialyte residue, H_2O_2 was chosen to promote the leaching process, because it was found to increase the oxidation potential of the system and affect the ionic forms of target elements. The addition of H_2O_2 increased the extractions of Zr and Nb but had no significant effect on Hf extraction. The results showed that 89.1% Zr, 81.2% Hf and 71.2% Nb can be recovered when employing the most suitable process parameters (Digestion conditions: H_2SO_4/eudialyte residue: 25 ml/100 g, water/eudialyte residue: 20 ml/100 g, 110 °C, 4 h; Leaching conditions: L/S: 3:1, H_2O_2/eudialyte residue: 10 ml/100 g, room temperature, 1 h). Using this process, the recovery yield of Zr was higher than that from any of the eudialyte concentrates that have been reported to date. The major phases formed after dry digestion were quartz and metal sulfates, and the phases found in the final residue after water leaching were quartz and some insoluble silicate phases.

Acknowledgments

Authors are thankful to EURARE project for providing the initial material. One of the authors (Yiqian Ma) is grateful to the Chinese Government for providing a scholarship.

References

Alonso, E., Sherman, A.M., Wallington, T.J.E., 2012. Valuating rare earth element availability: a case with revolutionary demand from clean technologies. Environ. Sci. Technol. 46 (6), 3406–3414.
Anthony, J.W., Bideaux, R.A., Bladh, K.W., Nichols, M.C., 2010. Handbook of Mineralogy. Mineralogical Society of America, Chantilly (VA20151–1110, USA.).
Aronniemi, M., Sainio, J., Lahtinen, J., 2005. Chemical state quantification of iron and chromium oxides using XPS: the effect of the background subtraction method. Surf. Sci. 578, 108–123.
Balomenos, E., Panias, D., Paspaliaris, I., Friedrich, B., Dittrich, C., et al., 2017. The EURARE project: development of a sustainable exploitation scheme for Europe's rare Earth ore deposits. Johnson Matthey Technol. Rev. 61 (2), 142–153.
Bayot, D., Devillers, M., 2006. Peroxo complexes of niobium(V) and tantalum(V). Coord. Chem. Rev. 250, 2610–2626.
Borst, A.M., Friis, H., Andersen, T., Nielsen, T.F.D., Waight, T.E., Smit, M.A., 2016. Zirconosilicates in the kakortokites of the Ilímaussaq complex, South Greenland: implications for fluid evolution and high-field strength and rare-earth element mineralization in Agpaitic systems. Mineral. Mag. 5–10.
Dai, Z., Dai, H., Zhou, Y., Liu, D., Duan, G., Cai, D., Li, Y., 2015. Monodispersed Nb_2O_5 microspheres: facile synthesis, air/water interfacial self-assembly, Nb_2O_5-based composite films, and their selective NO_2 sensing. Adv. Mater. Interfaces 2, 1500167.
Davris, P., Stopic, S., Balomenos, E., Panias, D., Paspaliaris, I., Friedrich, B., 2017. Leaching of rare earth elements from Eudialyte concentrate by suppressing silicon dissolution. Miner. Eng. 108, 115–122.
Dibrov, I.A., Chirkst, D.E., Litvinova, T.E., 2002. Experimental study of zirconium(IV) extraction from fluoride-containing acid solutions. Russ. J. Appl. Chem. 75 (2), 195–199.
Gao, Y., Masuda, Y., Ohta, Y., Koumoto, K., 2004. Room-temperature preparation of ZrO_2 precursor thin film in an aqueous peroxozirconium-complex solution. Chem. Mater. 16, 2615–2622.
Giuseppetti, G., Mazzi, F., Tadini, C., 1971. The crystal structure of eudialyte. Tschermaks Mineral. Petrogr. Mitt. 16, 105–127.
Golev, A., Scott, M., Erskine, P.D., Ali, S.H., Ballantyne, G.R., 2014. Rare earths supply chains: current status, constraints and opportunities. Res. Policy 41, 52–59.
Goodenough, K.M., Schilling, J., Jonsson, E., Kalvig, P., Charles, N., et al., 2016. Europe's rare earth element resource potential: an overview of REE metallogenetic provinces and their geodynamic setting. Ore Geol. Rev. 72, 838–856.
HSC Chemistry 6.0, 2006. Outokumpu Research Oy, License No: 60400.
Johnsen, O., Ferraris, G., Gault, R.A., Grice, J.D., Kampf, A.R., Pekov, I.V., 2003. The nomenclature of eudialyte-group minerals. Can. Mineral. 41 (3), 785–794.
Kazadi, D.M., Groot, D.R., Steenkamp, J.D., Pöllmann, H., 2016. Control of silica polymerisation during ferromanganese slag sulphuric acid digestion and water leaching. Hydrometallurgy 116, 214–221.
Khomyakov, A.P., Korovushkin, V.V., Perfiliev, Y.D., Cherepanov, V.M., 2010. Location, valence states, and oxidation mechanism of iron in eudialyte group minerals from Mössbauer spectroscopy. Phys. Chem. Miner. 37, 543–554.
Krishnamurthy, N., Gupta, C.K., 2015. The Rare Earths, Extractive Metallurgy of Rare Earths. CRC Press, pp. 1–84.
Kul, M., Topkaya, Y., Karakaya, I., 2008. Rare earth double sulfates from pre-concentrated bastnasite. Hydrometallurgy 93, 129–135.
Lebedev, V.N., 2003. Sulfuric acid technology for processing of eudialyte concentrate. Russ. J. Appl. Chem. 76 (10), 1559–1563.
Litvinova, T.E., Chirkist, D.E., 2013. Physic-chemical foundations of the eudialyte processing. In: Proceedings of the 2nd Russian Conference with International Participation New Approaches to Chemical Engineering Minerals. The Use of Extraction and Sorption, pp. 84–87.
Morais, C.A., Ciminelli, V.S.T., 2004. Process development for the recovery of high-grade lanthanum by solvent extraction. Hydrometallurgy 73, 237.
Sadeghi, M., Morris, G.A., Carranza, E.J.M., Ladenberger, A., Andersson, M., 2013. Rare earth element distribution and mineralization in Sweden: an application of principal component analysis to FOREGS soil geochemistry. J. Geochem. Explor. 133, 160–175.
Schilling, J., Wu, F.Y., McCammon, C., Wenzel, T., Marks, M.A.W., Pfaff, K., Jacob, D.E., Markl, G., 2011. The compositional variability of eudialyte-group minerals. Mineral. Mag. 75, 87–115.
Sjöqvist, A., et al., 2013. Three compositional varieties of rare-earth element ore: eudialyte-group minerals from the Norra Kärr alkaline complex, Southern Sweden. Fortschr. Mineral. 3 (1), 94–120.
Smith, R.M., Martell, A.E., 1998. NIST standard reference database. In: NIST Critically Selected Stability Constants of Metal Complexes Database, Version 5.0, National Institute of Standards and Technology (NIST). vol. 46.
Terry, B., 1983. The acid decomposition of silicate minerals part I reactivities and modes of dissolution of silicates. Hydrometallurgy 10, 135–150.
Vieceli, N., Nogueira, C.A., Pereira, M.F.C., Durão, F.O., Guimarães, C., Margarido, F., 2018. Recovery of lithium carbonate by acid digestion and hydrometallurgical processing from mechanically activated lepidolite. Hydrometallurgy 175, 1–10.
Voßenkaul, D., Birich, A., Müller, N., Stoltz, N., Friedrich, B., 2016. Hydrometallurgical processing of eudialyte bearing concentrates to recover rare earth elements via low-temperature dry digestion to prevent the silica gel formation. J. Sust. Metall. 1–11.
Yang, X., Zhang, J., Fang, X., 2015. Extraction kinetics of niobium by tertiary amine N235 using Lewis cell. Hydrometallurgy 151, 56–61.
Zakharov, V.I., Maiorov, D.V., Alishkin, A.R., Matveev, V.A., 2011. Causes of insufficient recovery of zirconium during acidic processing of lovozero eudialyte concentrate. Russ. J. Non Ferrous Metals 52 (5), 423–428.
Zhang, Y.D., Hua, Y.X., Gao, X.B., Xu, C.Y., et al., 2016. Recovery of zinc from a low-grade zinc oxide ore with high silicon by sulfuric acid curing and water leaching. Hydrometallurgy 166, 16–21.